Tellus (1986), *38A*, 178–188

Roughness elements of the sea surface—their spectral composition

By JIN WU, *Air-Sea Interaction Laboratory, College of Marine Studies, University of Delaware, Lewes, Delaware 19958, USA*

(Manuscript received March 12; in final form August 7, 1985)

ABSTRACT

The wind stress is considered to consist of momentum flux to aqueous flows and direct transfer to long waves. At various wind velocities, compositions of the wind stress and spectral contributions of wave components to each portion are presented. The rôle of the Charnock expression is further clarified, and all previous proposals relating roughness elements to waves are critically reviewed.

1. Introduction

Studies of air-sea interaction in the last two decades have evolved around a gross description of the wind-disturbed water surface with a roughness length. Limited attempts have been made to relate this length to the wave structure, while effort has been centered on its growth with wind velocity. Through an empirically determined growth function of the roughness length (Charnock, 1955; Wu, 1968), Wu (1969a) related the wind-stress coefficient to wind velocity and fetch and bypassed a more detailed study relating the roughness length to wave components. The time, however, appears to be ripe to examine the composition of roughness elements, and consequently to provide some insight into complex wind-wave interacting processes.

The wind stress has been known to consist of the shear stress supported by short waves (roughness elements) and the direct momentum flux to long waves. At various wind velocities, relative contributions of these two portions are estimated; the form drag on roughness elements is verified to be the major component. Spectral contributions of wave components to both portions of the wind stress are presented. The direct momentum flux to waves, following Phillips (1977), is related to the slope spectrum of the sea surface. The Charnock relation and the separation criterion (Wu, 1969b) are clarified to deal with only the momentum flux to aqueous flows through roughness elements. Previous results relating the roughness elements to sea-surface irregularities (Kondo et al., 1973), to wave spectrum (Kitaigorodskii, 1973; Donelan, 1982), and to slope spectrum of sea surface (Munk, 1955) are discussed.

2. Previous results

2.1 *Wind-stress coefficient and roughness length*

Wind velocity near the sea surface has been shown to follow the logarithmic profile (Wu, 1968):

$$U/u_* = (1/\kappa) \ln (z/z_0), \qquad (1)$$

where U is the wind velocity at elevation z above the mean sea surface; u_* is the wind-friction velocity, $u_* = (\tau/\rho)^{1/2}$, in which τ is the wind stress and ρ the density of air; $\kappa = 0.4$ is the von Karman constant; z_0 is the roughness length.

On the basis of available oceanic data, the wind-stress coefficient over the sea surface, C_{10}, was proposed (Wu, 1980) as

$$C_{10} = \tau/\rho U_{10}^2 = (0.8 + 0.065\, U_{10}) \times 10^{-3}, \qquad (2)$$

where U_{10} is the wind velocity measured at 10 m above the mean sea surface and expressed in *m/s*.

Among others, Garratt (1977) published a similar expression with slightly different coefficients, $C_{10} = (0.75 + 0.067U_{10}) \times 10^{-3}$. These small differences as well as those among other published formulas should not affect the main parameter – roughness length discussed in the present article.

It is generally accepted that the growth of the roughness length with wind velocity follows the Charnock (1955) equation. The latter with the recently determined (Wu, 1980) proportionality constant can be written as

$$z_0/(u_*^2/g) = a, \qquad a = 0.0185, \tag{3}$$

in which g is the gravitational acceleration, and a the so-called Charnock constant. This equation was first proposed purely on dimensional grounds, and was subsequently rationalized by Wu (1968) as an equation of state characterizing the equilibrium condition between the wind and waves, with gravity waves acting as roughness elements. Plotting z_0 versus u_*^2/g in logarithmic scales, the Charnock constant in eq. (3) was determined not only directly, instead of indirectly as customarily done from the wind-stress coefficient versus wind velocity diagram, but also with equal weights being effectively assigned to data points at all wind velocities.

2.2. *Wavelets and roughness elements*

Evidence of roughness elements composed of wavelets. The height of dominant waves in laboratory tanks was shown (Wu, 1970) to be comparable with that of roughness elements at high wind velocities, indicating that the airflow separates from dominant waves at high winds in the laboratory. The height of dominant waves, however, was shown (Wu, 1970) to be much greater than that of roughness elements in the ocean under all wind velocities, indicating that the airflow separates from short waves superimposed on dominant waves in the field. In summary, laboratory results have established the basis of identifying roughness elements, and oceanic results have indicated that the roughness elements are composed of wavelets.

Examining the concept that long waves do not act themselves as roughness elements but modify their density, measurements of the airflow boundary layer in a wind-wave tank were performed with and without pre-existing long waves (Wu, 1977). Provided that there is no airflow separation from long waves, their presence was found to reduce the density of roughness elements (ripples superimposing on long waves). Consequently, despite the fact that the height of dominant waves with the presence of pre-existing waves is much increased, the roughness length is reduced at low wind velocities and remains the same at high wind velocities.

Identification of dominant components of roughness elements. It was suggested (Wu, 1969b) that the airflow over a wind-disturbed water surface separates from the wavelet with its phase velocity smaller than the wind-friction velocity. This proposal with $c/u_* = 1$ as the criterion for flow separation is consistent with a subsequent laboratory study (Banner and Melville, 1976). These wavelets, therefore, act like roughness elements, of which the form drag supports a certain portion of the wind stress. The Charnock relation, suggested on dimensional grounds, and the separation criterion, established on physical evidence, were correlated earlier by Wu (1970). The correlation in turn lends further support to both the Charnock relation and the separation criterion.

Following a somewhat similar approach, Melville (1977) later also related the roughness elements to ripples with their phase velocity comparable with the wind-friction velocity. His argument, however, was based on the observation that the airflow separation occurs wherever the wave breaks. Although this observation was also involved in the proposed separation criterion (Wu, 1969b), the airflow separation is a phenomenon differing physically from wave breaking. Furthermore, we cannot establish that the separation occurs only when the wave breaks. We still prefer to relate the form drag to flow separation rather than wave breaking.

In all previous studies, the roughness length was related to the total wind stress, despite a generally accepted observation that a portion of the wind stress is transferred directly to long waves.

2.3. *Estimation of wave drag*

The wind stress actually consists of two portions, the momentum fluxes to aqueous flows and to waves. As discussed above, the former is the portion of the wind stress transmitted by the form drag due to the separation of air-flow from wavelets. The latter is the momentum flux extracted by long waves, the so-called wave drag (Stewart, 1961) due to the growth of waves in the wind direction.

The portion of the wave spectrum which receives most of the direct momentum flux from the wind is not as easy to identify as that which provides the form drag to the wind, since the former occurs over a much wider range of wave components than the latter. The direct momentum flux to waves, however, is generally considered to be governed by the ratio between the wave phase velocity and the wind-friction velocity. Experimental evidence cited by Phillips (1977) indicates that the contribution came mainly from the wave components in the range from the spectral peak with $c/U_{10} = 1$ to $c/u_* = 5$; the latter was considered to correspond to $c/U_{10} = \frac{1}{4}$. The portion of the momentum flux τ_w communicated to these wave components was then estimated by him to be about

$$\tau_w = 2.5 \times 10^{-2} \rho_a U_{10}^2 \overline{s^2} = 3.5 \times 10^{-4} \rho_a U_{10}^2, \quad (4)$$

where $\overline{s^2}$ is the mean-square slope of the sea surface. Assuming $C_{10} = 1.5 \times 10^{-3}$, Phillips reported $\tau_w/\tau = 0.23$.

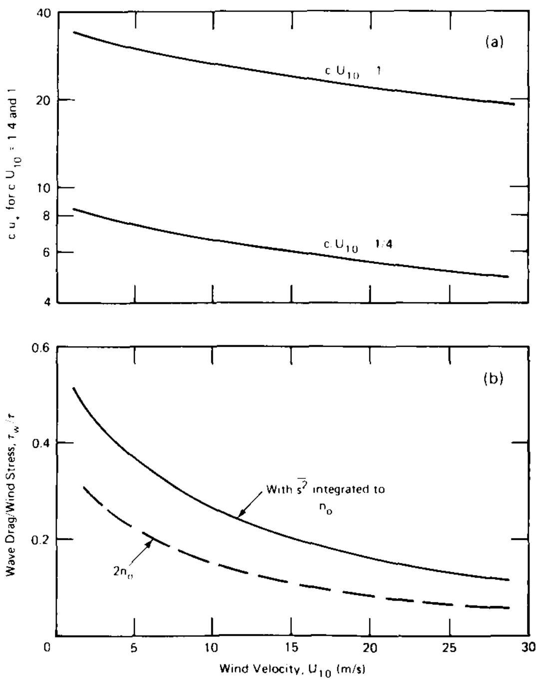

Fig. 1. Direct momentum fluxes to waves at various wind velocities.

3. Spectral contributions of wind stress

3.1. Direct momentum flux to waves

Following Phillips (1977), the mean-square slope can be obtained from the wave-number spectrum $\psi(\bar{k})$,

$$\overline{s^2} = \int k^2 \psi(\bar{k})\, \mathrm{d}\bar{k}, \quad (5)$$

where k and $\bar{k}$ are the wave number scalar and vector, respectively. Since the wave components which induce the wave drag are in the gravity range (Phillips, 1977), the integration in eq. (5) can be expressed (Phillips, 1977) as

$$\overline{s^2} = B \ln (k_c/k_o), \quad \text{with} \quad \psi(\bar{k}) = (B/\pi) k^{-4}, \quad (6)$$

where B is the spectral coefficient, k_o is at the spectral peak, and k_c corresponds to $c/u_* = 5$.

The values of c/u_* corresponding to both lower and upper limits of the integration used by Phillips (1977), $c/U_{10} = 1$ and $\frac{1}{4}$, can be obtained from eq. (2), and are shown in Fig. 1a. Since the upper limit used by Phillips is significantly different from $c/u_* = 5$, and since a more accurate formula for the wind-stress coefficient is now available, we proceeded to re-determine the ratio between the direct momentum flux to long waves and the wind stress as

$$\tau_w/\tau = (2.5 \times 10^{-2}/C_{10}) B \ln (k_c/k_o),$$
$$= (11.6 \times 10^{-5}/C_{10}) \ln (1/25\, C_{10}), \quad (7)$$

where $B = 4.64 \times 10^{-3}$ (Wu, 1972), $C_{10} = (u_*/U_{10})^2$, and $k_o = g/U_{10}^2$ were substituted. The above ratio is shown as a solid line in Fig. 1b, and is seen to decrease as the wind velocity increases. The results shown in the figure compare favorably with Phillips for most common wind velocities around U_{10} = 10 *m/s*, and with JONSWAP results (Hasselmann et al., 1973) for about the same velocity region as in Phillips. The magnitude and overall trend of the present estimate varying with the non-dimensional fetch also compare well with those reported by Snyder et al. (1981).

The scheme outlined above was considered by Phillips (1977) to provide a somewhat overestimate of the direct momentum flux to waves. He suggested that the equilibrium range might not extend to wave components traveling at approximately the same speed as the wind. In fact, there is evidence (Xu et al., 1984) indicating that for the frequency spectrum, the equilibrium range extends to as low as only twice the peak frequency. If we adopt their results, the corrected estimate is shown as a dashed line in Fig. 1b, where n_0 is the wave frequency at the spectral peak. The two lines in the figure are very likely the upper and lower limits of the estimated ratio, with the most probable value closer to the lower than to upper limit. In summary, although the present estimate, featuring that the fraction of momentum flux to waves varies with the wind velocity, differs from that of Phillips with the fraction remaining constant at all velocities, the basic conclusion that most of the wind stress is communicated to the water body, not to long waves, remains the same. This becomes even more obvious at high wind velocities with $\tau_w/\tau < \frac{1}{10}$.

3.2. *Refined correlation between Charnock expression and separation criterion*

Since the form drag on the roughness elements does not support all the wind stress, we should rewrite the Charnock relation as

$$z_r = a(ru_*^2)/g, \tag{8}$$

where $r = (\tau - \tau_w)/\tau$ is the ratio between the momentum flux to aqueous flows and the total wind stress, and z_r is used to distinguish it from z_0. The correlation (Wu, 1970) between the Charnock relation and the separation criterion can now be refined with eq. (8) and the new Charnock constant shown in eq. (3),

$$\begin{aligned} u_* &= (gz_r/ar)^{1/2} = [g(h/30)/0.0185r]^{1/2} \\ &= [g(\lambda/7)/0.56r]^{1/2} \\ &= (5/6r)(g\lambda/2\pi)^{1/2} = (5/6r)c = c, \end{aligned} \tag{9}$$

wherein the height of roughness elements h is considered to obey $h = 30z_0$ (Schlichting, 1968); the wave from which the airflow separates has the maximum steepness, $h/\lambda = \frac{1}{7}$ (λ is the wavelength); the phase velocity of waves follows the dispersion relation, $c = (g\lambda/2\pi)^{1/2}$; and the direct momentum transfer to waves is considered to be 10–20% of the wind stress with $r = \frac{5}{6}$.

In summary, although the partition of the wind stress to water body and to waves has long been recognized, the roughness length was still related to the total wind stress. Taking now the partition into consideration, we first clarify the physical concept by relating the roughness length to only the wave components wich provide form drag to the wind. This clarification then leads to a better correlation between the Charnock correlation and the separation criterion.

3.3. *Wind stress acting on wavelets*

As discussed earlier, the roughness elements are composed mainly of wavelets, whose phase velocity is the same as the wind-friction velocity. Wavelets with their phase velocity much smaller than u_* are not important, as the separation of airflows has already occurred over larger waves; waves with their phase velocity much greater than u_* are also not important, as there is no flow separation occurring over them. The wind-friction velocity can be calculated from the wind-stress coefficient given in eq. (2), while the phase velocity of waves can be calculated from (Lamb, 1932)

$$c = \left[\frac{g\lambda}{2\pi} + \frac{2\pi\sigma}{\rho_w\lambda}\right]^{1/2}. \tag{10}$$

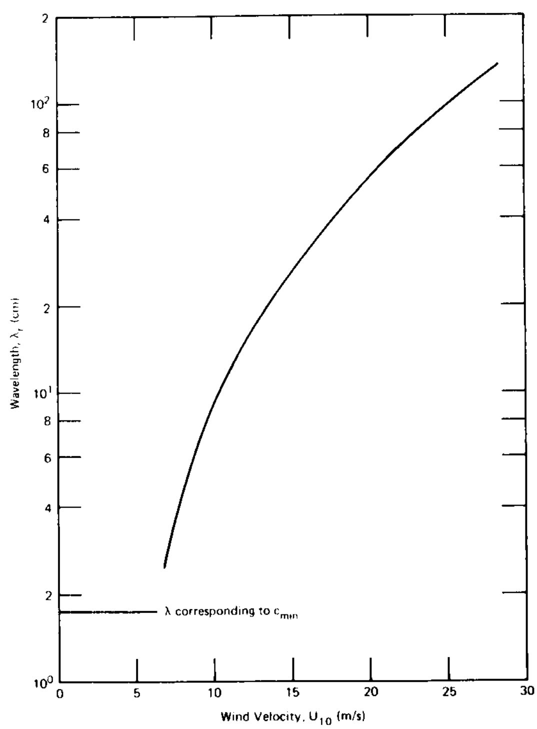

Fig. 2. Wavelengths of ripples acting as roughness elements at various wind velocities.

where σ is the surface tension, and ρ_w the density of water. Subsequently, we can obtain the length of wavelets satisfying the criterion $c/u_* = 1$. These wavelets are therefore the major contributor of roughness elements. The length of these wavelets, λ_r, is presented in Fig. 2. At low wind velocities, the criterion $c/u_* = 1$ cannot be satisfied; the length of waves having the minimum phase velocity (Lamb, 1932), $\lambda = 1.73$ cm for $c_{min} = 23$ cm/s, is shown in the figure. In summary, the procedure of identifying the critical wavelet is applicable for $U_{10} > 7$ m/s, where the wind-friction velocity is larger than c_{min}; therefore, no airflow separation should occur over wavelets. This result is very interesting, because at this very wind velocity, the atmospheric surface layer becomes aerodynamically rough (Wu, 1981).

3.4. Spectral representation of wind-stress components

As shown in Fig. 1b, a small fraction of the wind stress is transferred directly to long waves, while the major portion of the wind stress is supported by wave components satisfying $c/u_* = 1$. The latter is illustrated by the shaded area in Fig. 3. The detailed shape of the spectral contribution is unknown but the contribution should be from a very narrow region of c/u_*. The shaded area is centered around $c_{min} = 23$ cm/s for $U_{10} < 7$ m/s, and around $c = u_*$ for $U_{10} > 7$ m/s with u_* varying with wind velocity. The shaded area is illustrated in Fig. 3 to account for 80% of the wind stress, and is about 84% as indicated in eq. (9); this fraction, however, should vary with wind velocity as shown in Fig. 1b.

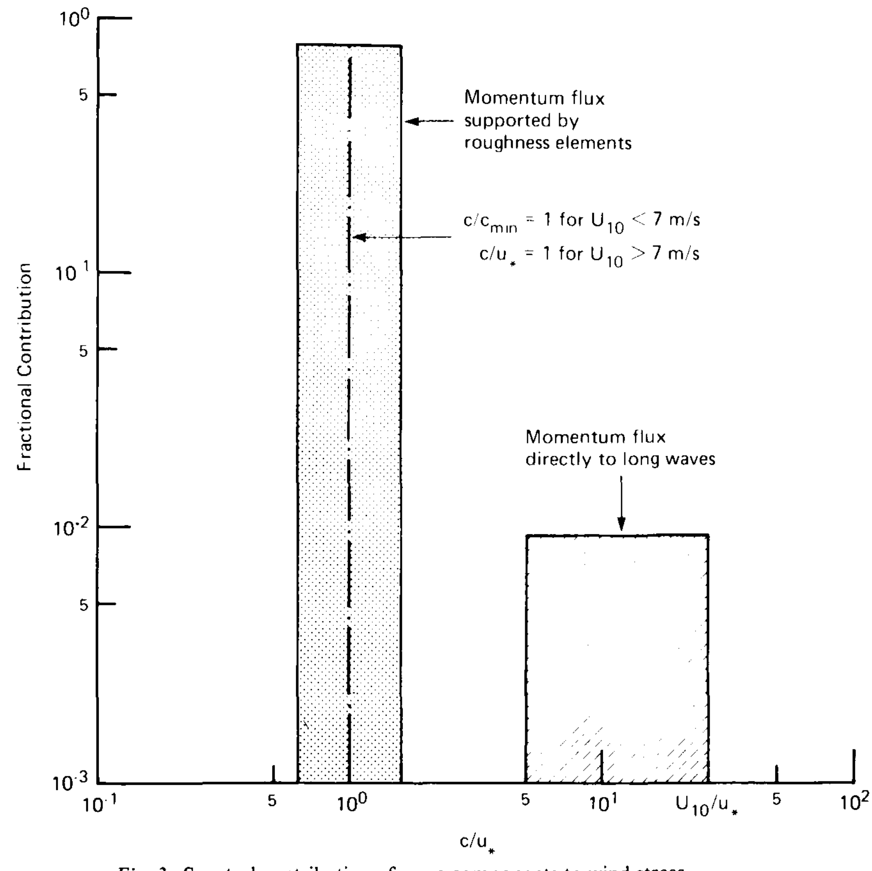

Fig. 3. Spectral contribution of wave components to wind stress.

For the portion of momentum flux from wind transferred directly to waves, the lower limit of wave components which contribute to this portion of the transfer has been considered to be $c/u_* = 5$, and the upper limit is $c/U_{10} = 1$ of which the corresponding value of c/u_* can be obtained from Fig. 1a. Accepting the wave-number spectrum $\psi(\bar{k}) = k^{-4}$, we have constructed the dashed area; the total contribution to the wind stress from wave components in this region is shown in Fig. 3 to be 20%, but again should vary with the wind velocity as shown in Fig. 1b. The contribution is about 16% according to eq. (9).

4. Discussion

4.1. Roughness height and wave spectrum

Kitaigorodskii and Volkov's Proposal. While the entire spectrum of surface waves has effects on the wind boundary layer, one portion of the spectrum, as discussed earlier, exerts more influence than the rest. Accessing relative contributions of various wave components in retarding airflows, Kitaigorodskii and Volkov (1965) suggested that the contribution of wave components to the roughness length is weighted by a factor, $\exp(-2\kappa c/u_*)$. Subsequently, Kitaigorodskii (1973) used the following expression to deduce the roughness height from the wave spectrum

$$h^2 = \int_0^\infty \phi(n) \exp(-2\kappa c/u_*)\, dn, \tag{11}$$

where as defined earlier, $h = 30z_0$ is the roughness height, and $\phi(n)$ the wave-frequency spectrum.

The high-frequency portion of the spectrum generally reaches a saturated state following $\phi(n) \sim n^{-5}$ (Phillips, 1977), while for deep-water waves we have $c = g/n$. Consequently, we can find the spectral composition of the roughness height shown in eq. (11) for any given wind velocity. In this case, the integrand I in eq. (11) varies with only the wave frequency, and has a bell-shaped distribution. The distribution for $U_{10} = 10$ m/s is shown in Fig. 4a, and the sharp drop-offs provide the justifications for using the spectrum and the dispersion relation cited above. The frequency n_p, at which the spectral contribution to the roughness height is peaked, can be found by differentiating I with respect to n; along with the dispersion relation, we have

$$n_p = \kappa g/5\pi u_* \quad \text{and} \quad c_p/u_* = 6.25, \tag{12}$$

where c_p is the phase velocity of the wave component n_p.

The narrow spectral contribution shown in Fig. 4a indicates that the main contribution of wave components to the roughness height is concentrated around the peak frequency n_p. The variations of the phase velocity c_p and the corresponding wave length λ_p with wind velocity are shown in Fig. 4b; these are seen to be associated with rather long waves propagating at high speeds. The $c_p/u_* = 6.25$ is also too large a value to be associated with roughness elements. In fact, these wave components have already been considered (Phillips, 1977) in the long-wave category, which abstracts a portion of the wind stress through the wave growth.

In summary, contrary to the discussion in Kitaigorodskii and Volkov, the roughness function proposed by them consists of long waves. It appears that their proposed weighting function favoring short waves is overwhelmed by the wave spectrum strongly favoring long waves.

Donelan's Proposal. More recently, Donelan (1982) took a somewhat different approach in relating roughness elements to the wave structure. He first considered, as in the above proposal, that all wave components contributed to the roughness length; subsequently, a weighting factor was applied to the resultant wind-stress coefficient, instead of individual wave components as illustrated in eq. (11). The factor applied by Donelan is the square of the ratio between relative velocity of the wave component with respect to the wind and the wind velocity. Because of this two-step correlation, it is very hard to evaluate, as has been done in the previous section, the relative contribution of individual wave components to the roughness length.

Overall, Donelan explained satisfactorily why the wind-stress coefficient is greater at a shorter fetch, where the ratio between the phase velocity of dominant waves and the wind velocity has a smaller value than that for the open sea. The conditions at short fetches were clearly Donelan's main concern; this is also evident from the data used for his correlation, showing that the height of

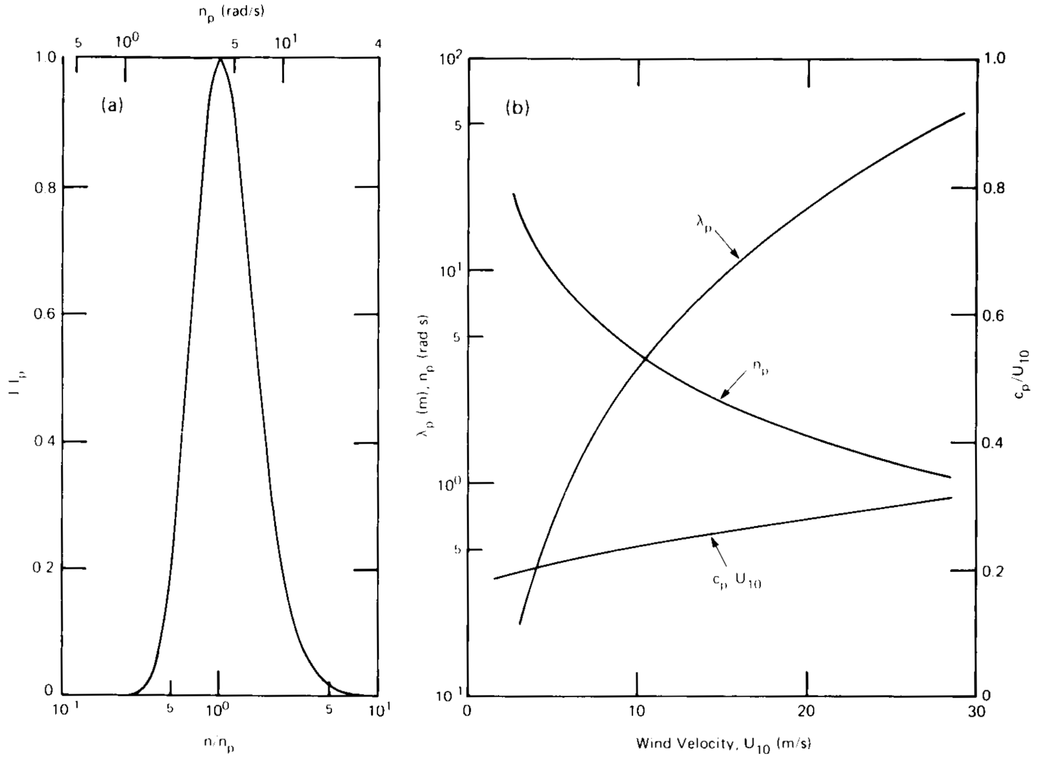

Fig. 4. Roughness composition proposed by Kitaigorodskii and Volkov (1965).

roughness elements ($30z_0$) approaches the height of dominant waves. The height of roughness elements in the open sea, conditions addressed in the present article, is only a small fraction of the wave height (Wu, 1970, 1980).

4.2. "Sea-surface irregularities" and roughness elements

Some interesting results on frequencies of occurrence of sea-surface irregularities, considered to support the wind stress, were reported by Kondo et al. (1973). They suggested that these irregularities are ocean waves of high frequencies 10–200 rad/s, and that the most frequently occurring height of irregularities (h_p) should correspond to the height of roughness elements. The wave-frequency range suggested by them and the frequency corresponding to $c/u_* = 1$ are compared in Fig. 5a. Wave components from a very narrow frequency band are proposed here to have a dominant contribution of roughness elements, while irregularities from a rather wide range were proposed by Kondo et al. In the present case, the wave component singled out is the longest from which the airflow separates, and all the shorter components are ineffective as the airflow has already separated from the longer one. In the case of Kondo et al., the most frequently occurring irregularities are selected, but it is unclear why the wave components near the high end of the frequency range act as effectively as those near the low end. As the wind velocity increases, longer (lower-frequency) wave components should become more important in provision of resistance to the airflow. This is reflected by the present results, while the proposal of Kondo et al. fails to respond; such is especially true for high wind velocities.

The representative heights determined by Kondo et al. were non-dimensionalized with u_*^2/g and are shown in Fig. 5b. If the irregularity and the roughness length are indeed similar, we should have approximately $h/(u_*^2/g) = 30a$ (Schlichting, 1968).

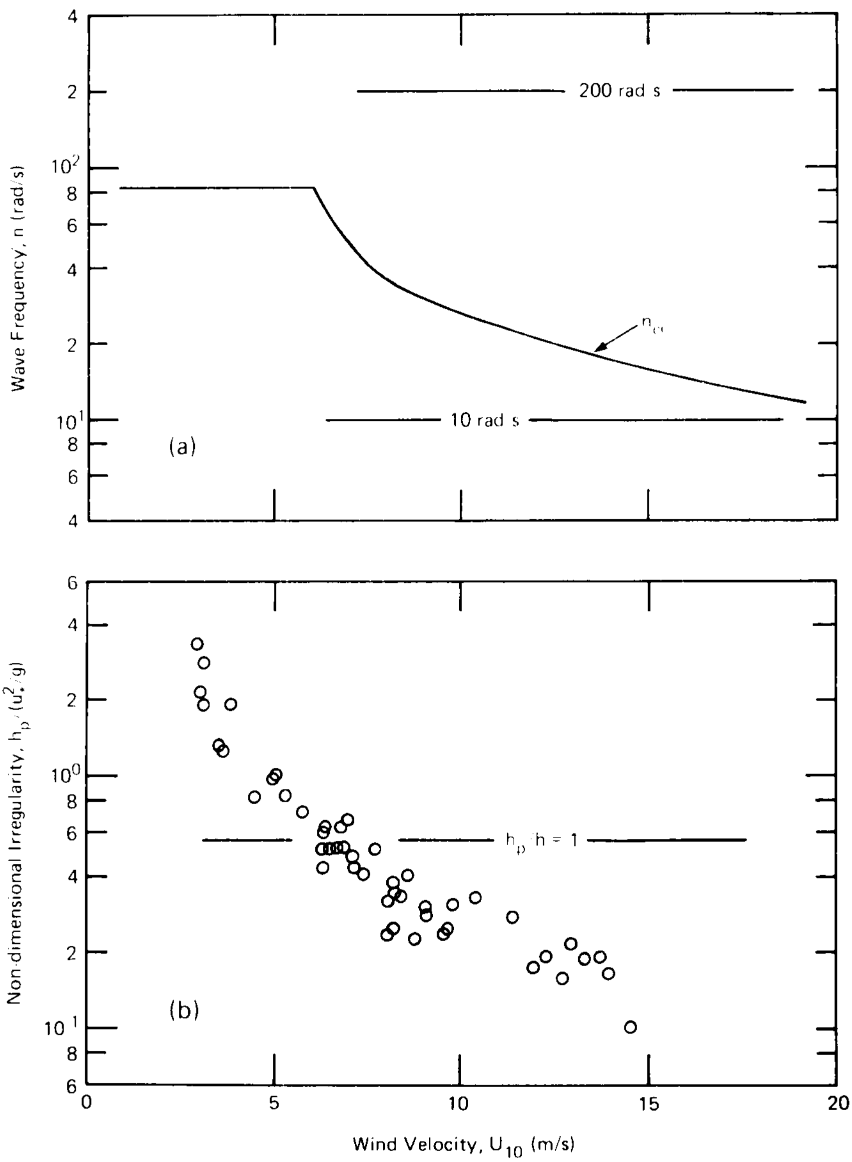

Fig. 5. Comparison of Kondo et al. (1973) and present proposals.

(The above relation $h/z_0 = 30$ established over the solid surface may need some modification over the sea surface; nonetheless, the modification, if there is any, should not be significant enough to affect the discussion associated with the results presented in Fig. 5b). However, the irregularities decrease continuously as the wind velocity increases. The two quantities h_p and h appear to be roughly comparable at approximately $U_{10} = 6.5$ m/s. Toward low wind velocities, the irregularity determined by Kondo et al. appears to over-represent the roughness length; toward high wind velocities, the irregularity under-represents the roughness length. This is essentially in line with the discussion in the previous paragraph regarding wave components proposed here and those by Kondo et al.

4.3. Mean-square slope and roughness length of sea surface

Because of their slow propagation and steep slope, short-wave components have long been recognized as the main contributors of roughness elements (Munk, 1955). For these wave components, the slope spectrum provides a better description than the height spectrum. Consequently, (Munk, 1955) attempted to correlate the roughness length, a statistical representation of roughness elements, with the mean-square sea-surface slope, a statistical description of ripple structures.

The wave-number spectrum for the capillary range was also proposed by Phillips (1977) to have the same shape as that for the gravity range but with a different spectral coefficient B' or

$$\psi(\bar{k}) = (B'/k)\,k^{-4}, \qquad k_\gamma < k < k_\nu, \tag{13}$$

where k_γ is the wave number dividing gravity and surface tension influences; k_ν is the neutrally stable wave number, correspond to the shortest wave which can be generated by the wind; the value of B' was found (Wu, 1972) to be 3.15×10^{-2}. Putting together eqs. (6) and (12), the growth of the mean square slope with wind velocity is illustrated in Fig. 6a, where the lower limit of the contribution comes from the spectral peak with $k_0 = g/U_{10}^2$, with the upper limit coming from k_ν. The variation of k_0 with U_{10} is straightforward and that of k_ν was discussed by Wu (1972); both variations are shown in Fig. 6b.

The expansion of the contribution shown in Fig. 6 from the dividing wave number k_γ to both lower and higher wave numbers with the increasing wind velocity describes well the growth of the mean-square slope. Furthermore, as illustrated in the figure, the growth is mainly from the capillary range. Both of these features appear to be in contradiction with the growth of the roughness length. For the latter, the growth should be mainly from the gravity range, with insignificant contribution from the capillary range.

4.4. Identifying regimes of the atmospheric surface layer

The regimes of the boundary layer are identified classically by the roughness Reynolds number, $R = u_* z_0/\nu$ (where ν is the kinematic viscosity of

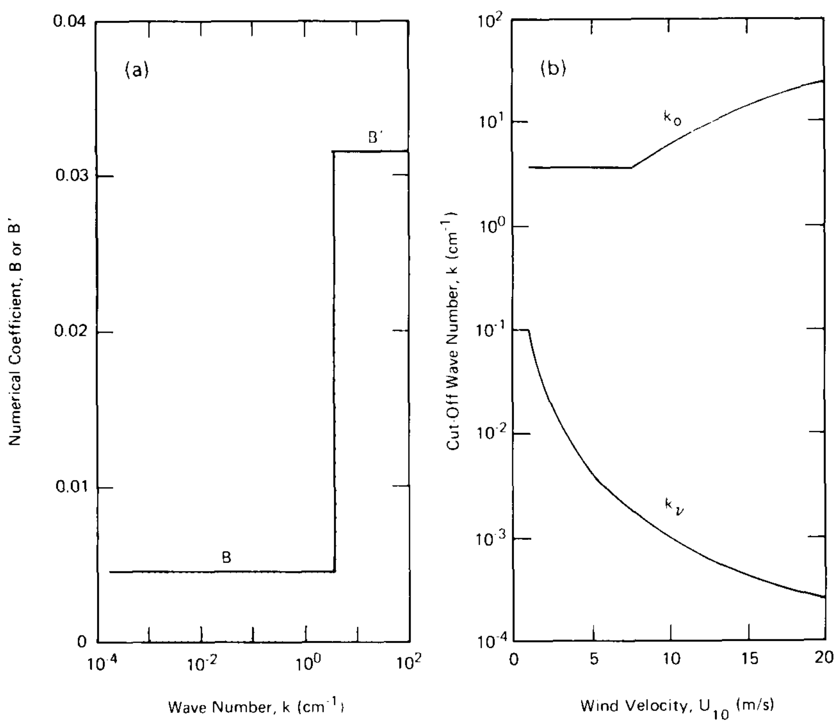

Fig. 6. Contributions to mean-square slope from various wave-number ranges.

air); the flow becomes aerodynamically rough for $R > 2.33$ (Schlichting, 1968). However, on the basis of detailed features of C_{10} varying with U_{10}, the atmospheric surface layer was identified as being aerodynamically rough when $R > 2.0$ occurs at $U_{10} = 7$ m/s (Wu, 1981).

The separation criterion discussed earlier indicates that the airflow separates from the wave component with its phase velocity smaller than the wind-friction velocity. The results shown in Fig. 2 demonstrate that this can take place only when the wind velocity is greater than 7 m/s. Below this wind velocity, all the wave components propagate at speeds greater than the wind-friction velocity. With the flow separation, the form drag on roughness elements supports the wind stress; the flow is aerodynamically rough. Without the flow separation, the wind stress can only be transmitted as the viscous shear stress; the flow is aerodynamically smooth. In summary, both sets of results indicate consistently that the atmospheric surface layer is aerodynamically rough for $U_{10} > 7$ m/s.

It was first suggested by Toba and Kunishi (1970) and subsequently by Melville (1977) that the atmospheric surface layer becomes aerodynamically rough when waves start to break. Although the laboratory results confirmed that the flow separation from dominant waves and their breaking occur concomitantly, the boundary layer is already aerodynamically rough before the occurrence of wave breaking. In fact, the criterion of airflow separation from waves was first proposed (Wu, 1969b) on the basis of this observation. In the field, the whitecaps were observed to incept at a much lower wind velocity, $U_{10} = 4$ m/s (Wu, 1982); this is much lower than 7 m/s discussed above.

5. Conclusion

The contributions of short waves and long waves to the wind stress have been further discussed and clarified. The short waves acting as roughness elements provide the resistance to airflows through the form drag on them. Only to this portion of the wind press, are the concept of describing the sea surface with a roughness length and the Charnock expression describing its growth with wind velocity, applicable. They should not be applied to the total wind stress, as is customarily done while recognizing the existence of direct momentum flux to long waves. In summary, the short waves propagate at speeds much slower than the wind velocity; from them the airflow separates. On the other hand, the long waves propagate at speeds much closer to the wind velocity, with a more effective momentum exchange between them and the wind. The momentum flux through short waves to aqueous flows is the major component of the wind stress, and its relative contribution increases with wind velocity. The direct flux to long waves is the minor component, and its relative contribution decreases as the wind velocity increases.

6. Acknowledgement

I am very grateful for the sponsorship of my work by the Fluid Dynamics Program, Office of Naval Research under Contract No. N000014-83-K-0316, and the Physical Oceanography Program, National Science Foundation under Grant No. OCE-8214998.

REFERENCES

Banner, M. L. and Melville, W. K. 1976. On the separation of air-flow over water waves. *J. Fluid Mech. 77*, 825–842.

Charnock, H. 1955. Wind stress on a water surface. *Q. J. R. Meteorol. Soc. 81*, 639–640.

Donelan, M. A. 1982. The dependence of the aerodynamic drag coefficient on wave parameters. First Int. Conf. on Meteor. and Air-Sea Interaction of the Coastal Zone, The Hague, Amer. Meteor. Soc., 381–387.

Garratt, J. R. 1977. Review of drag coefficient over ocean and continents. *Mon. Weather Rev. 105*, 915–929.

Hasselmann, K. et al. 1973. Measurements of wind wave growth and swell decay during the Joint North Sea Wave Project (JONSWAP). Herausgegeben von Deutsch. Hydrograph. Institut., Reihe A, no. 12.

Kitaigorodskii, S. A. 1973. The physics of air sea interaction. Israel Program for Scientific Translation.

Kitaigorodskii, S. A. and Volkov, Yu A. 1965. On the roughness parameter of the sea surface and the calculation of momentum flux in the near-water layer of the atmosphere. *Izv. Atmos. Oceanic. Phys. 1*, 973–988.

Kondo, J., Fujinawa, Y. and Naito, G. 1973. High-frequency components of ocean waves and their relation to the aerodynamic roughness. *J. Phys. Oceanogr. 3*, 197–202.

Lamb, H. 1932. *Hydrodynamics*, 6th edition. Cambridge University Press.

Melville, W. K. 1977. Wind stress and roughness length over breaking waves. *J. Phys. Oceanogr. 7*, 702–710.

Munk, W. H. 1955. Wind stress on water, a hypothesis. *Q. J. R. Meteorol. Soc. 81*, 320–332.

Phillips, O. M. 1977. *The dynamics of the upper ocean*, 2nd edition. Cambridge University Press.

Schlichting, H. 1968. *Boundary-layer theory*, 6th edition. McGraw-Hill.

Snyder, R. L., Dobson, F. W., Elliott, J. A. and Long, R. B. 1981. Array measurements of atmospheric pressure fluctuations above surface gravity waves. *J. Fluid Mech. 102*, 1–50.

Stewart, R. W. 1961. The wave drag of wind over water. *J. Fluid Mech. 10*, 189–194.

Toba, Y. and Kunishi, H. 1970. Breaking of wind waves and sea surface wind stress. *J. Oceanogr. Soc. Japan 26*, 71–80.

Wu, J. 1968. Laboratory studies of wind-wave interaction. *J. Fluid Mech. 34*, 91–112.

Wu, J. 1969a. Froude number scaling of wind-stress coefficients. *J. Atmos. Sci. 26*, 408–413.

Wu, J. 1969b. A criterion for determining airflow separation from wind waves. *Tellus 21*, 707–714.

Wu, J. 1970. Wind-wave interactions. *Phys. Fluids 13*, 1926–1930.

Wu, J. 1972. Sea surface slope and equilibrium wind-wave spectra. *Phys. Fluids 15*, 741–747.

Wu, J. 1977. Effects of long waves on wind boundary layer and on ripple slope statistics. *J. Geophys. Res. 82*, 1359–1362.

Wu, J. 1980. Wind-stress coefficients over sea surface near neutral conditions—A revisit. *J. Phys. Oceanogr. 10*, 727–740.

Wu, J. 1981. On critical roughness Reynolds number of the atmospheric surface layer. *J. Geophys. Res. 86*, 6661–6665.

Wu, J. 1982. Sea spray: a further look. *J. Geophys. Res. 87*, 8905–8912.

Xu, D., Wang, J. and Wu, J. 1984. On the saturation range of wind-wave spectrum from shallow to deep water. College of Marine Studies Tech. Rep. JW-24, University of Delaware.